

## Synthesis, characterization and conductivity measurements of polyaniline and polyaniline/fly-ash composites

Himanshu Narayan<sup>\*1</sup>, Hailemichael Alemu<sup>2</sup>, and Emmanuel Iwuoha<sup>3</sup>

<sup>1</sup> Department of Physics and Electronics, National University of Lesotho, Roma 180, Kingdom of Lesotho, Southern Africa

<sup>2</sup> Department of Chemistry and Chemical Technology, National University of Lesotho, Roma 180, Kingdom of Lesotho, Southern Africa

<sup>3</sup> Department of Chemistry, University of the Western Cape, Private Bag X17, Bellville 7535, South Africa

Received 23 June 2006, revised 17 August 2006, accepted 13 September 2006

Published online 24 October 2006

PACS 61.10.Nz, 72.80.Tm, 78.30.Jw, 81.05.Qk

Polyaniline (PANI) and polyaniline/fly ash (PANI/FA) composites with various concentrations of fly ash (20%, 40% and 50%) were synthesized by the process of *in-situ* polymerization. The samples were characterized by powder X-ray diffraction, thermogravimetric analysis, infrared spectroscopy, and scanning electron microscopy. Moreover, the dc conductivity of the samples was measured as a function of temperature in the range 80–290 K and it was found that the addition of FA decreases the conductivity. The temperature dependence of the dc conductivity for PANI and FA/PANI composites has been explained on the basis of the quasi one-dimensional variable hopping model. A very good agreement was found between the experimental data and the theory.

© 2006 WILEY-VCH Verlag GmbH & Co. KGaA, Weinheim

### 1 Introduction

Composites and blends based on conducting polymers (CP's) have recently emerged as a new class of potentially useful materials. A great deal of work is being done by many groups all over the world to understand and engineer their exceptional electrical, optical and chemical properties. In this direction, several classes of novel materials like, organic/CP [1], CP/CP [2] and CP/insulator [3] blends and composites, and more recently, inorganic/organic nanocomposites [4, 5] have been synthesized and studied in detail. Although still in their elementary stage, these investigations have revealed the immense possibilities of technological exploitation of these materials. What's more interesting is the fact that these materials also seem to have opened up a new field of research that could easily be considered as a link between polymers and nanoparticles.

Polyaniline (PANI) is one of the most interesting CP's, which is a suitable choice for various applications, such as, in solar cells, sensors, electromagnetic shields and rechargeable batteries' electrodes. Additionally, it is also known for its easy preparation methods and environmental stability [1, 2, 5–8]. Because of these unique properties, it has attracted special attention among all the CP's in the recent years.

Electrical conductivity of PANI can be significantly modified by suitable doping. For example, doping PANI with malonic acid increases its conductivity by an order of magnitude [1]. Similarly, nanocomposites made of PANI and montmorillonite show a variation in room-temperature conductivity as much as eight to nine orders of magnitude depending on the PANI content [4].

\* Corresponding author: e-mail: h.narayan@nul.ls, Phone: +266 2221 3521, Fax: +266 2134 0000

Fly ash (FA), which is otherwise a waste product obtained from the coal-furnaces, is another useful material that may be considered for doping in PANI. Being electrically insulating, the FA in its composite form with PANI, actually acts to regulate the conductivity of the material [3]. Effectively, it provides yet another method to modify the conductivity of PANI in order to achieve a desired result in view of a possible application. Moreover, since the processes involved in variation of conductivity of PANI and other conducting polymers are still not known in detail, a study of these materials is expected to throw some light on this aspect also.

In this paper, we present for the first time the results of thermogravimetric analysis (TGA) and dc-conductivity ( $\sigma_{dc}$ ) measurements on PANI-FA composites along with X-ray diffraction (XRD), infrared (IR) spectroscopy, and scanning electron microscopy (SEM) results.

## 2 Experimental

### 2.1 Synthesis of PANI/FA composites

The PANI/FA composites were synthesised according to the literature [3]. Aniline (AR) was purified by distillation before use and ammonium peroxydisulfate  $[(\text{NH}_4)_2\text{S}_2\text{O}_8]$ , HCl were used as received. A purified fine and fresh (FA) was collected from a local source. The compositions of FA are: silica, alumina, iron oxide lime magnesia and alkalis and different metallic and non-metallic elements [3, 8].

A 0.1 mol of aniline was dissolved in 1000 mL of 2 M HCl to form polyaniline (PANI). Varied wt% amount of FA powder (20, 40, 50) was added to the PANI solution with vigorous stirring. A 0.1 mol  $(\text{NH}_4)_2\text{S}_2\text{O}_8$  aqueous solution was added slowly with continuous stirring, which acts as the oxidant. The reaction mixture was agitated continuously for another 8 hrs keeping the solution in an ice bath. The precipitate formed was collected by filtration and washed with distilled water and acetone until the filtrate became colourless and free from aniline and  $\text{SO}_4^{2-}$ . The filtrate was dried at room temperature. The prepared PANI/FA composites contained 20%, 40%, and 50% by weight of FA in PANI.

### 2.2 Measurements

X-ray powder diffraction (XRD) measurements were done with a Shimadzu D5000 diffractometer (from Shimadzu, Japan) using  $\text{Cu K}_\alpha$  radiation ( $\lambda = 1.5406 \text{ \AA}$ ). Thermogravimetric experiments were carried out with SDT 2960 Simultaneous DSC-TGA, TA Instruments, in static air (with no air flow). Approximately 12 mg of each sample were analyzed between 30 and 750 °C at flow rate of 10 °C  $\text{min}^{-1}$  using alumina crucibles. The FT-IR spectra of the samples were obtained with a Nicolet MAGNA-IR 760 Spectrometer in the range 4000–400  $\text{cm}^{-1}$ . The samples were prepared as pellets using KBr. Moreover, scanning electron microscopy (SEM) was carried out using JSM 5600 electron microscope (from Jeol Ltd., Japan).

For the conductivity measurements, the powder sample was pressed into small pellets by using about 10 tons of pressure with a cold-press. The pellets so formed were brittle and therefore they were left for a week at room temperature so that they become hard enough for cutting. Then the pellets were cut into parallelepiped shapes and mounted on a four-probe dipstick resistivity set up one by one. Electrical connections for current and voltage probes were made using silver paste and the stick was dipped into a liquid nitrogen dewar. The resistance of the samples was measured during warming up of the sample as the dipstick was pulled up gradually from the dewar, from about 80 K up to room temperature (290 K). After the measurements, the dc-conductivity  $\sigma_{dc}(T)$  was calculated from the resistance data.

## 3 Results and discussion

### 3.1 X-ray diffraction

Figure 1 shows the XRD results for pure PANI and for PANI-FA composites with increasing concentrations, viz., 20%, 40% and 50% weight-percentage. Pure PANI shows a characteristic XRD peak at

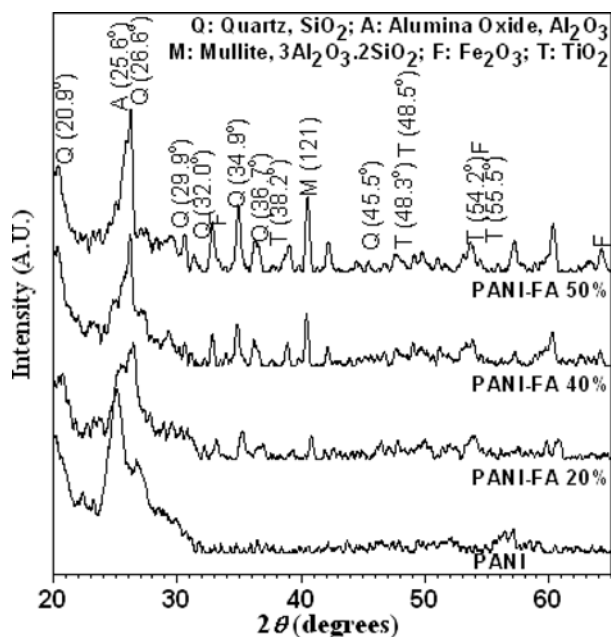
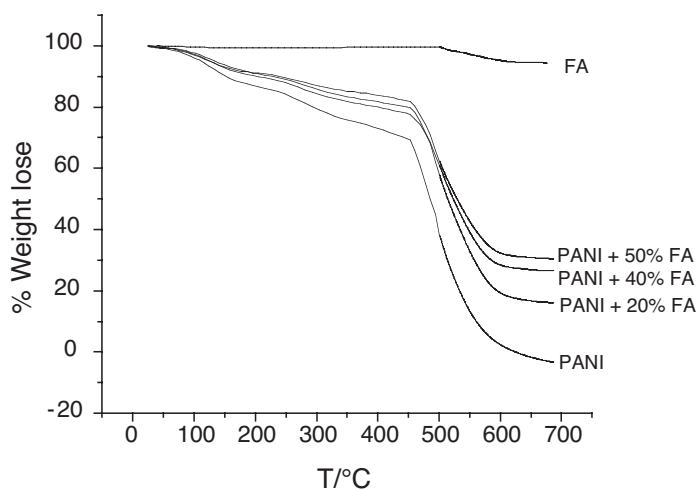


Fig. 1 X-ray diffraction pattern of PANI–FA composites with different FA concentrations.

$2\theta = 25.9^\circ$ , that corresponds to the emeraldine salt (ES-I) phase of the polymer [9, 10]. Crystalline phases of quartz ( $\text{SiO}_2$ ), alumina oxide ( $\text{Al}_2\text{O}_3$ ) and mullite ( $3\text{Al}_2\text{O}_3 \cdot 2\text{SiO}_2$ ) are three main constituents of FA, which also contains amorphous phases of these materials along with some other oxides. Therefore, the XRD pattern of PANI-FA composites shows the semi-crystalline nature of the material. As reported earlier by Raghavendra et al. [3], the PANI–FA composites show a sharp peak at  $2\theta = 26.6^\circ$ , which is evident in our XRD results (Fig. 1). As the FA concentration increases, the height of  $25.9^\circ$  PANI peak gradually diminishes and a peak around  $2\theta = 26.1^\circ$ , increases and becomes more prominent. This new peak is essentially a combination of the PANI peak ( $2\theta = 25.9^\circ$ ) and the peaks due to the constituents of FA around the same  $2\theta$  value. For example, two main constituents of FA, namely, quartz and alumina oxide peak at  $26.6^\circ$  and  $25.6^\circ$ , respectively [one more constituent, titanium oxide ( $\text{TiO}_2$ ) also peaks at  $2\theta = 25.8^\circ$ , although its weight percentage present in FA is insignificant when compared to that of quartz and alumina oxide]. Therefore, as the FA concentration increases, the PANI peak gradually disappears. In the XRD plots, this occurs as a gradual shift of peaks near  $2\theta = 25.9^\circ$  towards slightly higher  $2\theta$  values.

### 3.2 Thermogravimetric analysis

The thermal behaviour of the FA and the different PANI/FA samples was investigated by thermogravimetry (TG) and the results are shown in Fig. 2. The steady weight loss observed for the PANI/FA samples in the temperature range  $80\text{--}450^\circ\text{C}$  is attributed to the elimination of adsorbed water (up to 30%) from both the oxide and polymer surface and acid dopant [11–13]. In this temperature range, there is no observed weight loss for the FA sample. In addition to this, a well-differentiated behaviour marked by a strong weight loss in the temperature range  $470\text{--}600^\circ\text{C}$  are observed for PANI and PANI/FA composites. This attributes to the degradation of the skeletal polyaniline chain structure [11–13]. In this temperature range the FA sample also exhibits a relatively small weight losses (about 6%), which is mainly due to the complete burning off carbon in the fly ash [14]. Using the TG data, a plot of % weight loss versus % FA added in PANI gave a straight line with correlation coefficient of 0.990 indicating a good ratio of FA to PANI in the synthesised samples. Based on the TG data, the amount of polyaniline in each sample was assigned, corresponding to the following (in weight percent): 100.0; 83.9; 73.5; 69.6 for the



**Fig. 2** Thermogravimetric curves obtained in air atmosphere at  $10\text{ }^{\circ}\text{C min}^{-1}$  for: FA; PANI + 50 wt% FA; PANI + 40 wt% FA; PANI + 20 wt% FA; PANI.

samples: PANI; 20% FA in PANI; 40% FA in PANI and 50% FA in PANI samples respectively. The above values are reasonably acceptable since a certain amount of the added FA in each sample would be expected not to form precipitate with PANI.

### 3.3 Infrared spectroscopy

Figure 3 shows the IR spectra of PANI and 40 wt% FA in PANI. The characteristic peaks observed at the spectrum of PANI are due to the quinoid ring absorption at  $1630$  and  $1150\text{ cm}^{-1}$ , absorption of benzoquinone at  $885\text{ cm}^{-1}$ , the absorption due to benzenoid at  $1375$  and  $1500\text{ cm}^{-1}$ , and the broadband for the N–H stretching at  $3400\text{--}3100\text{ cm}^{-1}$  [3, 15]. These absorption bands are clear indications of the existence of the quinoid and benzenoid rings in the polymer chain. The bands at  $1630$  and  $1150\text{ cm}^{-1}$  are characteristic of the emeraldine salt (ES-I) form of PANI (as observed from the XRD also). The presence of these peaks also indicates that the emeraldine salt is composed of quinoid and benzenoid moieties

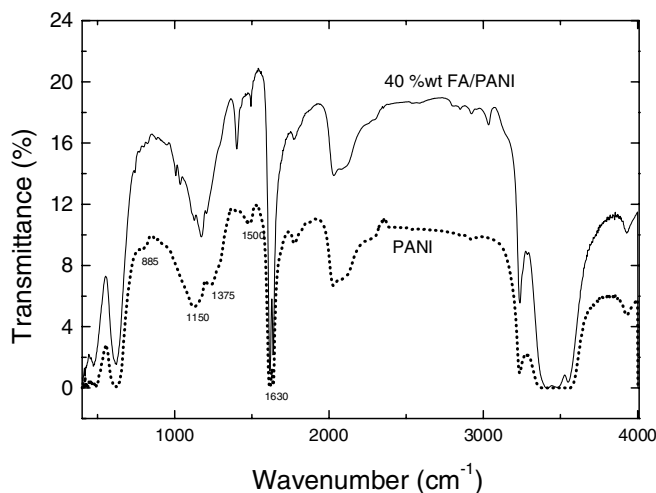


**Fig. 3** Infrared spectra of PANI and PANI + 40 wt% FA.

[15–18]. The intense and sharp band at  $1630\text{ cm}^{-1}$  further indicates the relative abundance of the quinoid ring in the polymer structure. The IR spectrum of the FA/PANI composite in most of the cases resembles that of PANI indicating the existence of PANI in the emeraldine salt form. Slight shifts and additional peaks are observed in the range  $2500\text{--}3000\text{ cm}^{-1}$ ;  $1300\text{--}1500\text{ cm}^{-1}$  and  $1100\text{--}1300\text{ cm}^{-1}$ . The shifts and the additional characteristic peaks may be attributed to the presence of silica and metal oxides present in FA. The IR spectrum of FA (spectrum not shown) gave a very broad peak in the range  $1500\text{--}400\text{ cm}^{-1}$ . The broadening of the peak could be due to the merging of the IR peaks that arise from the absorption of the various metal oxides present in FA [3]. The IR spectra of 20 wt% FA in PANI and 50 wt% FA in PANI do not exhibit much variation in the characteristic peaks.

### 3.4 Scanning electron microscopy

SEM was recorded for two different magnifications, i.e.,  $1000\times$  and  $10000\times$ . Figure 4 (a) shows a typical scanning electron micrograph of pure PANI at  $10000\times$  magnification. It is apparent from the picture that the material is homogeneous with the particle size ranging from  $4\text{ }\mu\text{m}$  to  $10\text{ }\mu\text{m}$ , with most of the particles around  $5\text{--}6\text{ }\mu\text{m}$  size. It may also be noted from the SEM that the bigger particles are agglomerations of smaller, well-connected grains. The good connectivity among grains is expected to facilitate good electrical conductivity in this sample.

The SEM of the PANI–FA composites with 20 wt%, 40 wt% and 50 wt% of FA at the same magnification of  $10000\times$  are shown in Fig. 4(b), (c) and (d), respectively. From the SEM pictures, it is evident

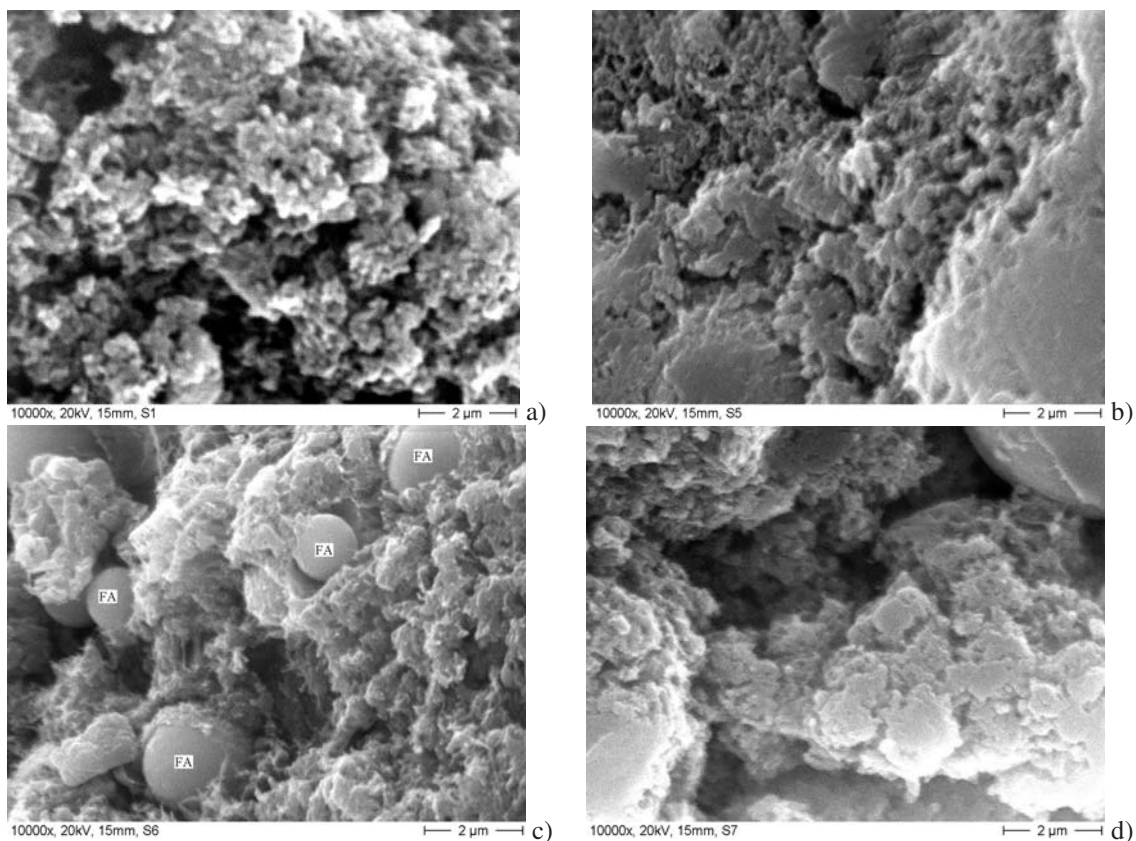


**Fig. 4** SEM pictures of PANI–FA composites. (a) Pure PANI. (b) PANI + 20 wt% FA. (c) PANI + 40 wt% FA (the cenospheres are clearly seen in this micrograph). (d) PANI + 50 wt% FA.

that granularity increases with addition of FA in PANI, although the pure PANI appears to be more granular (at 10000 $\times$ ) than the composites. The spherical FA particles (cenospheres) [3] of 1–2  $\mu\text{m}$  size may also be seen clearly in Fig. 4(c). Moreover, the grain size seems to decrease as the FA concentration increases. For example, in the composite with 20 wt% FA, the grains are much bigger than the scale in the SEM, i.e., 20  $\mu\text{m}$ , whereas in the composite with 50 wt% FA, the size ranges from a few microns to about 10  $\mu\text{m}$ . Again, the bigger particles seem to be agglomerates of smaller grains. This may also be looked upon as the decreasing grain-connectivity with increasing FA concentration in these composites. Effectively, it should be expected that the electrical conductivity decreases with increasing FA concentration.

### 3.5 Electrical conductivity

The conductivity  $\sigma_{\text{dc}}(T)$  for pure PANI and two different compositions of PANI-FA composites is shown in Fig. 5 for the temperature range 80–290 K. It may be noted from the graph that  $\sigma_{\text{dc}}$  of pure PANI as well as that of the composites increases with increasing temperature showing their semiconducting nature. The value of temperature coefficient of resistivity (TCR) for pure PANI around room-temperature as calculated from our plots is  $-2.8 \times 10^{-3} \Omega \text{ cm K}^{-1}$  at 0–10  $^{\circ}\text{C}$  range, which is comparable with a reported value of  $-4.0 \times 10^{-3} \Omega \text{ cm K}^{-1}$  at 20–30  $^{\circ}\text{C}$  range [19]. However, considering the difference of temperature ranges, the value of TCR calculated from our graph is slightly lower than what was expected. Nevertheless, the conductivity of PANI was found to be 4.17  $\text{S cm}^{-1}$  around 285 K (12  $^{\circ}\text{C}$ ), which is in very good agreement with the reported average value of 4.37  $\text{S cm}^{-1}$  at 20  $^{\circ}\text{C}$  [19].

It may be easily noted from Fig. 5 that the conductivity decreases with the increasing concentrations of FA. For the composites with 20 wt% and 40 wt% of FA in PANI, the values of  $\sigma_{\text{dc}}$  around room temperature (285 K) are 0.81  $\text{S cm}^{-1}$  and 0.21  $\text{S cm}^{-1}$ , respectively. The TCR calculated from the plots for the composites are  $8.6 \times 10^{-3} \Omega \text{ cm K}^{-1}$  and  $3.5 \times 10^{-2} \Omega \text{ cm K}^{-1}$ , respectively, for the 20 wt% and 40 wt% of FA in PANI. Evidently, as expected, the TCR as well as the room temperature resistivity increases (conductivity decreases) with the addition of FA in PANI.

In order to explain the temperature dependent conductivity behaviour of our samples, we assume that polymer chains are extended through the disordered regions and they connect the ‘crystalline islands’. In

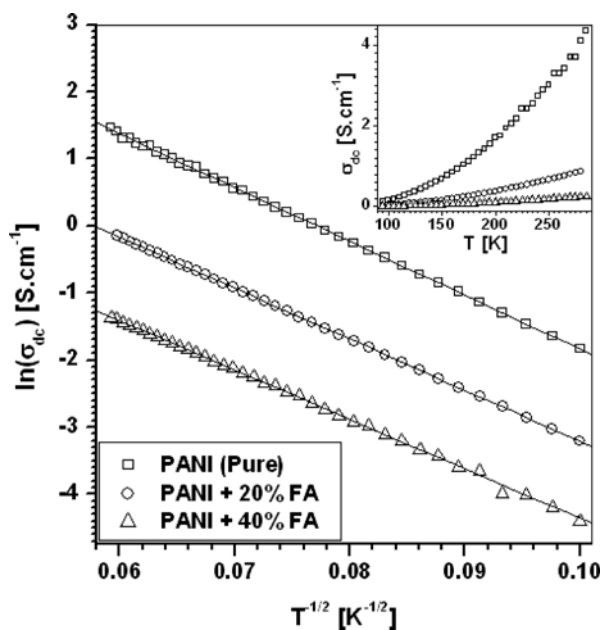


**Fig. 5** Temperature dependence of dc electrical conductivity ( $\sigma_{\text{dc}}$ ). The solid lines show the best-fit according to the expression (1) (see text). The inset shows the experimentally determined values of  $\sigma_{\text{dc}}$  as a function of temperature.

this picture, charge carriers may diffuse along the electrically isolated disordered chains but are always capable to get localized because of the 1D nature of the chains. In such a situation, the temperature dependence of  $\sigma_{dc}$  for PANI and the composites may be explained on the basis of the quasi one-dimensional variable hopping (quasi 1D VRH) model [4, 20–22]. Within the framework of this model,  $\sigma_{dc}$  is given by the relationship

$$\sigma_{dc} = \sigma_0 \exp \left[ - \left( \frac{T_0}{T} \right)^\gamma \right], \quad (1)$$

with the value of  $\gamma \approx 0.5$  for 1D hopping ( $\gamma \approx 0.33$  for 2D hopping, and  $\gamma \approx 0.25$  for 3D hopping). Here, the quantity  $\sigma_0$  is also temperature dependent, but its dependence may be neglected when compared to the stronger dependence of the exponential term.  $T_0$  is given by the relationship

$$k_B T_0 = \frac{16}{L_{\parallel} N(E_F) z}. \quad (2)$$

In this expression,  $L_{\parallel}$  is localization length,  $N(E_F)$  is the density of states at Fermi level,  $z$  is the number of nearest-neighbour chains. Effectively,  $T_0$  is the energy barrier for electrons to hop between localized states.

To fit our experimental  $\sigma_{dc}$  data (Fig. 5) for PANI (pure), we have used the reported value of  $T_0 = 6400$  K [21] in Eq. (1). As evident from the figure, a very good agreement was found between experimental data and the theoretical straight line. For the composites with 20 wt% and 40 wt% of FA in PANI, however, the best fit was achieved by using the value of  $T_0$  equal to 6500 K and 6700 K, respectively. This increase in  $T_0$  is expected with increase of FA percentage in PANI. Since  $T_0$  is inversely proportional to the localization length  $L_{\parallel}$ , it means that as the FA percentage increases,  $L_{\parallel}$  for the charge carriers in the composites decreases. As a result, the charge carriers become more localized, and thus are less free to move. Consequently, the conductivity decreases with increasing FA concentrations. In terms of  $T_0$ , this means that addition of FA in PANI increases the energy barrier required for hopping of electrons, and thus making the conduction less easier. Therefore, it may be concluded that the quasi one-dimensional hopping is the mechanism responsible for electrical conductivity in PANI/FA composites.

## 4 Conclusions

Conducting polyaniline and fly ash/polyaniline composites were synthesized by *in-situ* polymerization and characterized by X-ray diffraction, thermogravimetric, infrared, SEM and dc conductivity techniques. The XRD pattern of pure PANI showed the presence of the emeraldine salt (ES-I) phase of the polymer and that of the PANI/FA composites showed the semi-crystalline nature of the material. As the concentration of FA increased in the composites, a small gradual shift of peaks around  $2\theta = 25.9^\circ$  towards higher  $2\theta$  values was also observed. This may be attributed to the merging of the ES-I peak with those due to the FA constituents, which peak around the same value of  $2\theta$ . The thermogravimetry curves showed a clear and marked difference between PANI, FA, FA/PANI composites, where the major weight losses were associated with the degradation of the skeletal polyaniline chain structure. The TG analysis enabled us to assign the weight percent of PANI in each synthesized sample. Infrared spectra of PANI and FA/PANI composites indicated the existence of the quinoid and benzenoid rings in the polymer chain of PANI. These spectra also supported the XRD result that the polymer used in this work was the emeraldine salt (ES-I) form of PANI. The SEM pictures of the FA/PANI composites showed the increase in granularity with addition of FA in PANI and the existence of the spherical FA particles (cenospheres). From the study of dc conductivity as a function of temperature, it was inferred that both the pure PANI as well as the PANI/FA composites were semiconducting in nature. Moreover, the conductivity was found to decrease with the addition of FA in PANI. The observed temperature behaviour of conductivity of PANI as well as that of PANI/FA composites was explained on the basis of quasi one-dimensional variable range hopping model. Thus it was concluded that the conductivity in PANI/FA composites is due to the quasi one-dimensional hopping, and therefore, the decrease of conductivity with the addition of FA may be attributed to the localization of charge carriers.

**Acknowledgement** One of the authors (HN) would like to thank Mr Anthony Matobo for his technical help during conductivity measurements.

## References

- [1] M. Karakişla, M. Saçak, E. E. Erdem, and U. Akbulut, *J. Appl. Electrochem.* **27**, 309 (1997).
- [2] A. Raghunathan, P. K. Kahol, J. C. Ho, Y. Y. Chen, Y. D. Yao, Y. S. Lin, and B. Wessling, *Phys. Rev. B* **58**, R15955 (1998).
- [3] S. C. Raghavendra, S. Khasim, M. Revanasiddappa, M. Prasad, and A. B. Kulkarni, *Bull. Mater. Sci.* **26**, 733 (2003).
- [4] D. Lee, K. Char, S. W. Lee, and Y. W. Park, *J. Mater. Chem.* **13**, 2942 (2003).
- [5] D. C. Schnitzler and A. J. G. Zarbin, *J. Braz. Chem. Soc.* **15**, 278 (2004).
- [6] B. C. Roy, M. Dutta Gupta, L. Bhowmik, and J. K. Ray, *Bull. Mater. Sci.* **24**, 389 (2001).
- [7] B. C. Roy, M. Dutta Gupta, L. Bhowmik, and J. K. Ray, *Bull. Mater. Sci.* **26**, 633 (2003).
- [8] S. C. Raghavendra, R. L. Raibagkar, and A. B. Kulkarni, *Bull. Mater. Sci.* **25**, 37 (2002).
- [9] J. P. Pouget, M. E. Jdzefowicz, A. J. Epstein, X. Tang, and A. G. MacDiarmid, *Macromolecules* **24**, 779 (1991).
- [10] A. Wolter, P. Rannou, J. P. Travers, B. Gilles, and D. Djurado, *Phys. Rev. B* **58**, 7637 (1998).
- [11] K. Pielichowski, *Solid State Ion.* **104**, 123 (1997).
- [12] E. S. Matveeva, R. D. Calleja, and V. P. Parkhutik, *Synth. Met.* **72**, 105 (1995).
- [13] M. G. Han, Y. J. Lee, S. W. Byun, and S. S. Im, *Synth. Met.* **124**, 337 (2001).
- [14] A. Arenillas, K. M. Smith, T. C. Drage, and C. E. Snape, *Fuel* **84**, 2204 (2005).
- [15] S. H. Nalwa (Ed.), *Handbook of Organic Conductive Molecules and Polymers*, Vol. 2 (John Wiley and Sons, New York, USA, 1997), pp. 506–537.
- [16] I. Hazada, Y. Furukawa, and F. Ueda, *Synth. Met.* **29**, 303 (1989).
- [17] Y. Cao, *Synth. Met.* **35**, 319 (1990).
- [18] Y. Cao, P. Smith, and A. J. Heeger, *Synth. Met.* **32**, 263 (1989).
- [19] J. Stejskal and R. G. Gilbert, *Pure Appl. Chem.* **74**, 857 (2002).
- [20] Z. H. Wang, E. M. Scherr, A. G. MacDiarmid, and A. J. Epstein, *Phys. Rev. B* **45**, 4190 (1992).
- [21] F. Zuo, M. Angelopoulos, A. G. MacDiarmid, and A. J. Epstein, *Phys. Rev. B* **36**, 3475 (1987).
- [22] A. B. Kaiser, *Rep. Prog. Phys.* **64**, 1 (2001).